

Na behaviour in shock-induced melt phase of the Yanzhuang (H6) chondrite

CHEN MING and XIE XIANDE

Guangzhou Institute of Geochemistry, Chinese Academy of Sciences,
510640 Guangzhou, China

Abstract: The Yanzhuang meteorite was severely shocked and reheated in an extraterrestrial impact event; it consists of four shock facies characteristic of disequilibrium shock effects. This study reveals that the volatile element Na in the shock-induced melt phase is not unequivocally depleted. Na preservation in the melt phase could correspond to: (1) high shock pressures (≥ 30 GPa) and high post-shock temperatures that acted in most parts of the meteorite, resulting in reduced rock porosity and lower pressure and temperature gradients between the melt phase and the surrounding shock facies. (2) quenching of melt phase (6 - 400°C/s). Na redistribution in the melt phase is shown here: (1) Na concentrated to Fe-Ni-S melt at high pressure and high temperature. Fe-Mn-Na phosphate, a possibly new phase, was formed in the metal-troilite eutectic nodules. (2) Minor amounts of Na were solidified into the recrystallized low-Ca pyroxene, thus resulting in a slightly enhanced Na content in the pyroxene. (3) Part of the Na was "frozen" into the silicate melt glass.

Key-words: Na-behaviour, shock facies, melt phase, Yanzhuang chondrite.

Introduction

It is well known that melt veins and pockets in ordinary chondrites are heavily shock-metamorphosed areas which have experienced very high pressures and temperatures. Although they are produced from localized *in-situ* melting of chondrites, they are basically of chondritic composition. It seems inevitable that shock-induced melting would result in the loss of some volatile elements by vaporization during cooling of the melt. Evident Na loss from shock veins has been reported in several L and H chondrites. Among the L6 chondrites, losses of 25-35 % Na are reported in the veins of Apt and Vouillé (Dodd & Jarosewich, 1982) and 30 % Na in the early vein of Chantonay (Dodd *et al.*, 1982). Semenenko *et al.* (1992) stated that the veins in the Barbotan (H5) and Charsonville (H6) chondrites have lost 46 % and 50 % Na, respectively, in contrast to their unmelted chondritic hosts.

The Yanzhuang (H6) chondrite is a Chinese meteorite fall that has been severely shocked and reheated (Xie *et al.*, 1991, 1994). The meteorite contains abundant melt veins and melt pockets. However, no significant loss of Na or other volatile non-noble gas elements have been found in the melt phase. The mineralogical study shows that sodium redistribution had taken place in the melt phase. We report here the results of an investigation of the shock facies and Na behaviour within the melt phase.

Samples and experimental methods

The sample was cut from the largest fragment (823 g) of Yanzhuang. Several polished thin sections containing both melt phase and unmelted chondritic areas were prepared for petrology, mineralogy and microprobe analyses. Among the

four shock facies distinguished in this meteorite, 1.5 g of each facies was extracted and ground into powder, from which a 200 mg subsample of each facies was used for compositional determination by instrumental neutron activation analysis (INAA).

Thin sections were studied by optical microscopy and scanning electron microscopy (SEM). Semi-quantitative energy dispersive chemical analyses (EDX) were conducted on a SEM equipped with an EDX accessory. An ARL-SEMQ automated electron probe microanalyser was employed for elemental quantitative analyses (EPMA). Operating conditions were 15 kV accelerating potential and 25 nA sample current. The element contents were calculated from the X-ray data using ZAF correction.

Results and discussion

1. Shock facies

The Yanzhuang meteorite presents four shock facies characteristic of disequilibrium shock effect (Fig.1): (1) Slightly deformed chondritic host with poorly defined chondrule structure. The mechanical deformation of minerals of this facies is intense, resulting in numerous olivines displaying strong undulatory extinction, 4 to 5 sets of planar fractures, mosaic texture with domains of 10-15 μm and more than 3-4° of rotation. Some plagioclases have been transformed to maskelynite. This facies make up about 40 % by volume of the meteorite. (2) Brecciated areas. Most minerals of this facies, especially the silicates, have been heavily deformed and broken into fragments. Most plagioclases have been transformed to maskelynite. The fragments of olivine display intense mosaic texture with domains a few microns across with more than 5 to 8° of rotation. This facies makes up about 20 % by volume of the meteorite. (3) Blackened and partially melted chondritic areas. These areas occur in neighbouring melt veins and melt pockets. All plagioclase here was melted, while troilite, metal and pyroxene were partially melted. Solid state recrystallization of olivine and pyroxene grains has occurred extensively. Some melted metal and troilite has penetrated into the fractures of the silicates, thus resulting in blackening of these areas. This facies make up about 10 % by volume

of the meteorite. (4) Melt phase including melt veins and pockets. Melt veins and melt pockets, which connect with each other and penetrate the whole meteorite make up about 30 % of the meteorite. The widths of melt veins range from 0.1 to 15 mm, while one large melt pocket has a volume of 24 cm^3 . The melt phase mainly consists of recrystallized microcrystalline olivine and low-Ca pyroxene, recrystallized olivine and pyroxene fragments, silicate melt glass and metal-troilite eutectic nodules with dendritic textures.

2. Chemical composition

Both the melt phases and the unmelted chondritic areas of Yanzhuang were identified by INAA to have nearly identical compositions in major, minor and trace elements (Chen, 1992; Begemann *et al.*, 1992; Chen *et al.*, 1994). Table 1 shows that the contents of most volatile elements (such as Na, K, Zn and Se) are very similar in the melt phase and the unmelted chondritic areas, thus indicating that these elements were not measurably affected by shock. The Na content of the melt phase is not significantly depleted in contrast with other shock facies of this meteorite and with average H chondrite falls (6380 ppm). Minor differences of Na content (< 15 %) among different shock facies and among the measurements from different laboratories could be due to sample selection and experimental conditions.

3. Mineralogy of the melt phase

Pyroxene

The melt phase in the Yanzhuang chondrite contains a number of microcrystalline pyroxenes. They range from 1 to 10 μm in size and have euhedral and subhedral forms surrounded by silicate melt glass. Both high-Ca and low-Ca pyroxenes are encountered, while low-Ca pyroxene is predominant. Table 2 and Fig. 2 show that the low-Ca pyroxene in the melt phase is heterogeneous from grain to grain in contrast to the homogeneous compositions of low-Ca pyroxenes in the chondritic host. These microcrystalline pyroxenes contain high concentrations of Al_2O_3 , Cr_2O_3 , CaO and Na_2O , (e.g. 0.1 - 2.7 wt.% Al_2O_3 , 0.1 - 1.3 wt.% Cr_2O_3 , 0.7 - 4.5 wt.% CaO

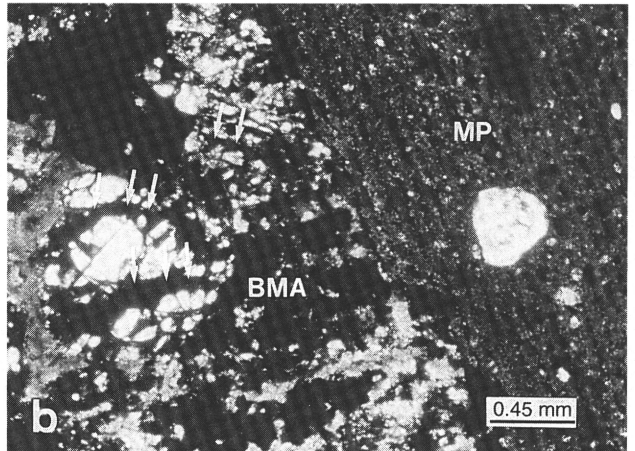
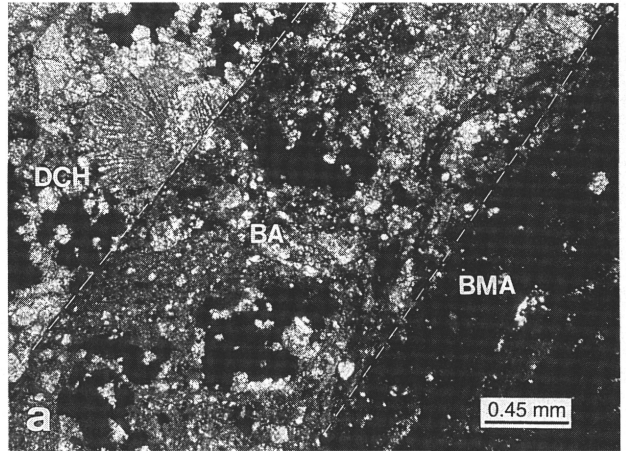


Fig. 1. The Yanzhuang chondrite has been heavily shocked and reheated. It consists of four shock facies: (1) slightly deformed chondritic host (DCH) in which poorly defined chondrule structures can still be discerned (Fig. 1a); (2) brecciated areas (BA) in which most minerals have been heavily damaged and fragmented (Fig. 1a); (3) blackened and partially melted chondritic areas (BMA) in which silicates and metal minerals were partially melted (Fig. 1a & b). Fig. 1b also shows some melted metal and troilite (arrows) penetrating into the fractures of pyroxenes and olivines, thus resulting in the blackening of these areas; (4) melt phase including melt pockets (MP) and melt veins (MV) which consist of microcrystalline olivine and pyroxene, recrystallized olivine and pyroxene fragments, metal-troilite eutectic nodules and silicate melt glass (Fig. 1b and c). Plane polarized transmitted light.

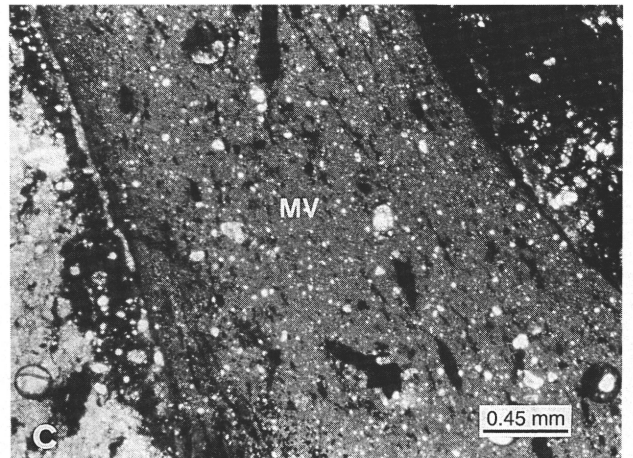


Table 1. Na concentrations of shock facies of the Yanzhuang chondrite determined by INAA.

	A	B	C	D (melt	E phase)	Average H chondrite fall
			(ppm)			
(1)	7020	6010	6600	6440	6820	
(2)	6310(±640)			5940	(±500)	
(3)	6040(s.d.=3)			6370	(s.d.=3)	
(4)						6380

Note: A = Lightly deformed chondritic host; B = Brecciated area; C = Blackened and partially melted chondritic area; D = Melt vein; E = Melt pocket. Melt phase includes D and E.

(1) This study. Note that one measurement of each facies was conducted and no standard deviation of these measurements has been estimated.

(2) Y. Chen et al (1994).

(3) F. Begemann et al. (1992).

(4) E. Jarosewich (1990).

and up to 0.19 wt.% Na₂O). Semenenko & Golovko (1994) also reported similar compositional features in the low-Ca pyroxenes of the melt veins of the Barbotan, Charsonville and Pervomaisky chondrites. Considering these compositional characteristics, the low-Ca pyroxenes could have crystallized from shock-induced mixed silicate melts.

Olivine

Microcrystalline olivine in the melt phase has similar occurrence features as microcrystalline

pyroxene. However, these olivines have the same composition as the olivine of the chondritic host (Table 2), and only small numbers of grains contain slightly high CaO (up to 0.28 wt.%).

Phosphates in metal-troilite eutectic nodules

Metal-troilite eutectic nodules in the melt phase of Yanzhuang are from 0.1 to 10 mm in diameter, thus indicating a local Fe-Ni-S fractionation in the shock-induced melt. A number of phosphate inclusions were found within troilite in these nodules, occurring as fine-grained

Table 2. Chemical compositions of low-Ca pyroxenes and olivines in the Yanzhuang chondrite determined by EPMA.

	Low-Ca pyroxene				(wt.%)	Olivine			
	Host* (6)	s.d.	Melt † (14)	s.d.		Host* (8)	s.d.	Melt † (7)	s.d.
Na ₂ O	0.02	0.01	0.07	0.06	n.d.	-	n.d.	-	
CaO	0.68	0.04	1.39	0.97	0.05	0.02	0.08	0.08	
MgO	30.79	0.56	30.28	1.65	42.49	0.86	41.96	0.45	
FeO	10.96	0.32	10.19	0.54	16.76	0.26	16.92	0.89	
MnO	0.47	0.02	0.41	0.04	0.45	0.01	0.43	0.02	
Al ₂ O ₃	0.23	0.07	0.73	0.66	n.d.	-	0.03	0.03	
Cr ₂ O ₃	0.15	0.05	0.76	0.40	0.10	0.04	0.08	0.13	
V ₂ O ₃	n.d.	-	0.04	0.06	n.d.	-	n.d.	-	
TiO ₂	0.17	0.06	0.11	0.06	0.04	0.03	n.d.	-	
SiO ₂	56.24	0.51	54.84	1.28	38.71	0.35	38.69	0.49	
Total	99.71		98.82		99.61		98.19		

Host* = chondritic host.

Melt † = melt phase.

() = number of analyses.

s.d. = standard deviation.

n.d. = not detected.

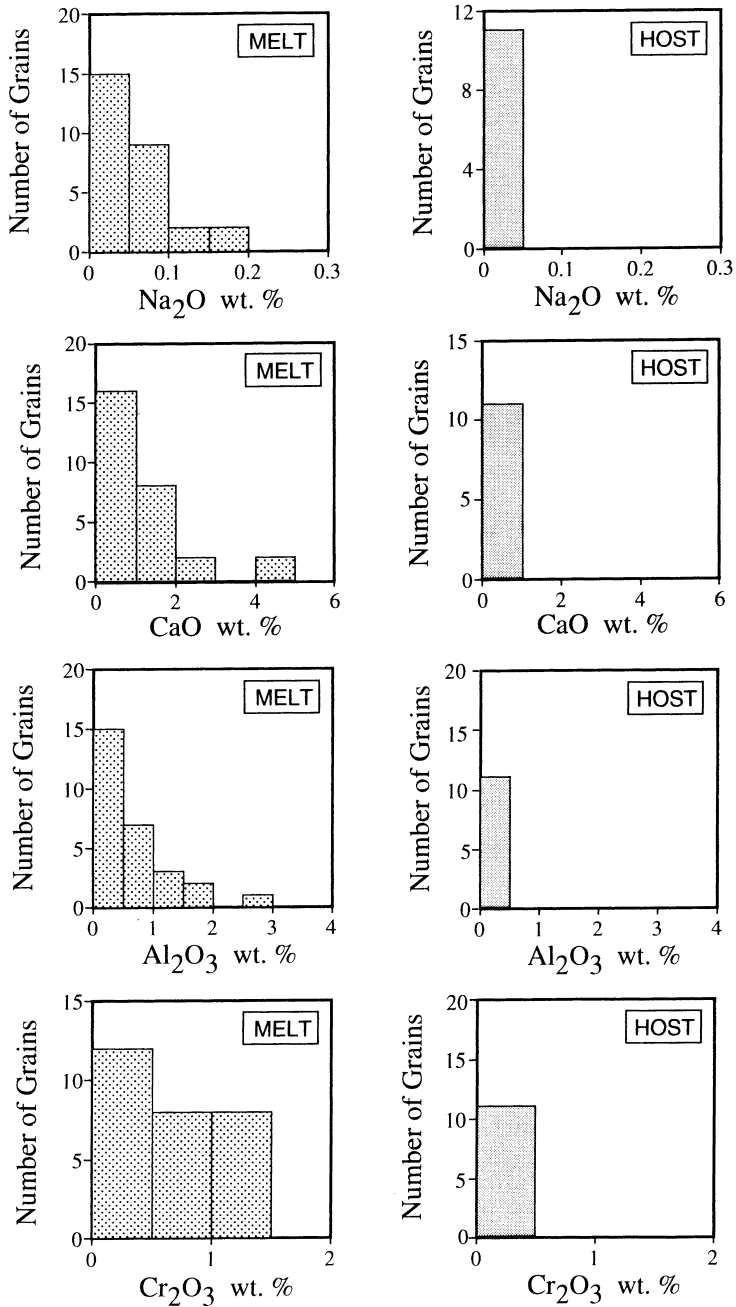


Fig. 2. Compositional characteristics of low-Ca pyroxenes. The diagrams show the frequencies of CaO, Cr₂O₃, Al₂O₃ and Na₂O contents of low-Ca pyroxenes in the melt phase (Melt) and in the chondritic host (Host). Low-Ca pyroxenes in the melt phase have heterogeneous compositions and many grains contain higher contents of Al₂O₃, Cr₂O₃, CaO and Na₂O than the low-Ca pyroxenes of the chondritic host. The low Ca-pyroxenes in the chondritic host have homogeneous composition.

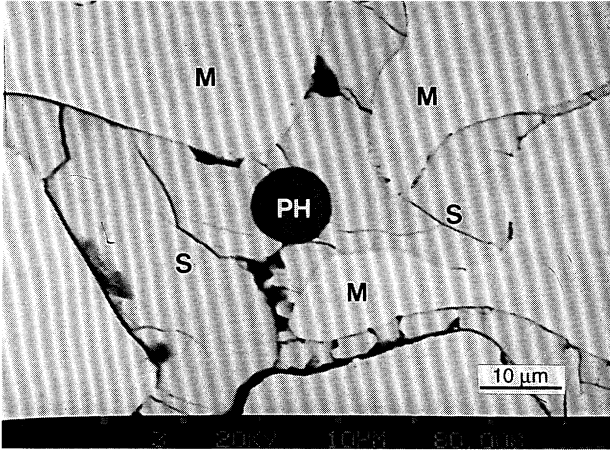


Fig. 3. Back-scattered electron image showing a Fe-Mn-Na phosphate inclusion (PH) within troilite (S) of a metal-troilite eutectic nodule in a melt pocket. The Na content of this phosphate inclusion was measured to be about 4 wt.%. Iron-nickel metal is designated as M.

spherules 2 to 8 μm in diameter (Fig. 3), and containing 48 to 58 wt.% FeO, 2 to 5 wt.% MnO and up to 4.55 wt.% Na_2O (Table 3, Fig. 4). Na contents of the phosphates show positive correlation with Ca and K. Analysis of Mn, K, Na, and Ca contents in the inclusions indicates a homogeneous compositional distribution.

Among the identified phosphate inclusions,

only a few grains were found to have the composition of graffonite $(\text{Fe}_{2.95}\text{Mn}_{0.05})_3(\text{PO}_4)_2$. The majority of the other phosphate grains contain Fe, Mn and Na. The Na contents of these grains range from 1.32 to 4.55 wt.% Na_2O which show a continuum of compositions (Fig. 4). Na-rich Fe-Mn phosphates (≥ 4 wt.% of Na_2O) have the approximate formula $(\text{Na,Ca,K})_2(\text{Fe,Mn})_8(\text{PO}_4)_6$.

Table 3. Chemical compositions of phosphates in the metal-troilite eutectic nodules determined by EPMA.

No.	Na_2O	K_2O	CaO	MgO	FeO	MnO	Cr_2O_3	SiO_2	P_2O_5	Total
	(wt.%)									
1	n.d.	n.d.	n.d.	n.d.	57.93	2.39	0.18	0.03	38.88	99.41
2	1.32	n.d.	0.10	0.02	55.49	2.36	0.18	0.15	38.48	98.09
3	1.59	n.d.	n.d.	n.d.	54.37	3.75	0.45	0.08	38.12	98.38
4	2.07	n.d.	0.03	n.d.	53.97	3.48	0.31	0.23	39.58	99.66
5	2.38	n.d.	0.06	0.04	54.27	2.23	0.17	0.18	38.86	98.17
6	2.55	n.d.	0.02	n.d.	53.21	3.03	0.33	0.10	38.84	98.08
7	2.67	n.d.	0.10	0.03	53.24	2.73	0.20	0.15	39.23	98.45
8	2.78	n.d.	0.02	n.d.	52.15	4.26	0.53	0.17	39.15	99.06
9	2.84	n.d.	0.14	0.09	53.23	2.51	0.29	0.34	39.04	98.46
10	2.95	0.07	0.19	0.06	50.30	4.25	0.34	0.18	39.31	97.65
11	3.19	n.d.	0.13	0.08	52.64	3.11	0.10	0.53	38.00	97.77
12	3.21	0.02	0.32	0.07	51.18	3.20	0.39	0.25	39.27	97.90
13	3.24	0.02	0.03	n.d.	52.62	3.73	0.37	0.33	39.65	99.89
14	3.25	0.03	0.19	0.10	51.26	3.88	0.53	0.35	38.76	98.35
15	3.28	n.d.	0.23	0.06	49.78	4.90	0.39	0.39	38.86	97.90
16	3.57	0.06	0.30	0.14	49.12	3.60	0.64	1.05	40.03	98.51
17	3.57	0.06	0.38	0.06	50.87	3.13	0.49	0.20	39.63	98.39
18	3.72	0.04	0.37	0.12	51.09	2.71	0.27	0.56	38.70	97.59
19	4.02	0.08	0.46	0.22	50.07	2.85	0.40	0.72	39.28	98.09
20	4.07	0.03	0.40	0.08	50.68	3.41	0.32	0.41	39.42	98.82
21	4.55	0.10	0.41	0.12	48.79	4.00	0.84	0.38	39.73	98.92

Note that the chemical compositions were measured from 21 grains of phosphates (No.1 to 21). In these analyses, grain No.1 is free of Na, other grains (No.2 to 21) contain 1.32 - 4.55 wt.% of Na_2O .

n.d.= not detected.

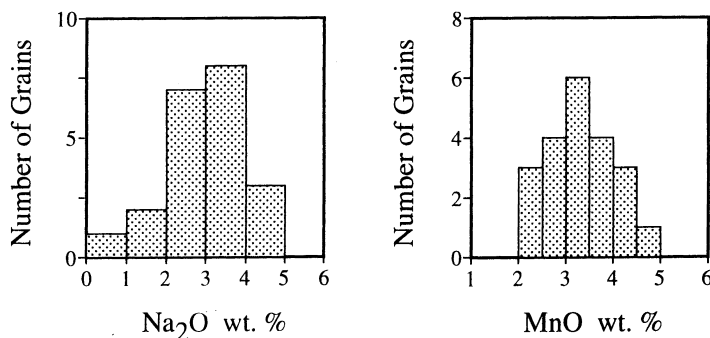


Fig. 4. Compositional characteristics of phosphates. The diagrams show the frequencies of Na₂O and MnO contents of the analysed phosphate grains. Na₂O and MnO concentrations in different grains are heterogeneous.

It would be desirable to conduct structural analyses of these phosphates by X-ray diffraction if some sufficiently large grains could be located. Based on the principles of crystal chemistry, Fe and Mn in the lattice cannot be substituted by Na, Ca and K. Therefore, it is reasonable to consider that the Fe-Mn-Na phosphate (Na,Ca,K)₂(Fe,Mn)₈(PO₄)₆ could be a new phase. If this is the case, Na-bearing Fe-Mn phosphates (1.32-3.72 wt.% of Na₂O) would represent a mixture of graptoneite and Fe-Mn-Na phosphate. It is possible that the single phase of Fe-Mn-Na phosphate in the Na-bearing Fe-Mn phosphate inclusions is too small to be resolved by microprobe.

The predominant phosphate in the Yanzhuang chondrite is whitlockite, which occurs as an accessory mineral and contains only up to 3 wt.% Na₂O. According to our observation, phosphate inclusions occurring in the kamacite, taenite and troilite of the chondritic areas have not been identified. During shock events, the chondrite is melted and volatile elements, such as Na and P released from the decomposed whitlockite and plagioclase, are concentrated into the shock-induced Fe-Ni-S melt at high pressures and high temperatures. P combines with the Fe, Mn and Na, to form phosphate which occurs as inclusions within the troilite.

Fe-Mn phosphates usually do not occur in ordinary chondrites (Fuchs, 1969). Olsen & Steele (1993) reported the discovery of Fe-Mn-Na phosphate (Na,K)₂(Fe,Mn)₈(PO₄)₆ within troilite nodules of the IIIAB iron meteorites. They provisionally referred to this phosphate as 2:8:6 phosphate because no X-ray data have yet been obtained. Olsen & Steele (1994) suggested a model to explain the formation of such phosphates: after Fe-phosphate formation, Mn, Na, K, Ca diffuse into them forming Mn-bearing

graptoneite and 2:8:6 phosphate. The Fe-Mn-Na phosphate in Yanzhuang should correspond to the 2:8:6 phosphate found in IIIAB iron meteorites by Olsen & Steele (1993), in view of the similarity of composition and occurrence of phosphates. However, it should be emphasized that the phosphates in Yanzhuang were formed during a shock event.

4. Silicate melt glass

The melt phase of Yanzhuang contains about 3-5 % silicate melt glass occurring among the recrystallized olivine, pyroxene, metal and troilite. TEM study indicates that the areas of melt glass are generally less than 1 mm across (Chen, 1992), which is too small to allow microprobe analysis. EDX measurement shows that the melt glass has very a heterogeneous composition with 50-90 wt.% SiO₂, 3-15 wt.% Al₂O₃, 0.5-15 wt.% FeO, 0.5-30 wt.% MgO, 1-5 wt.% Na₂O, 1-4 wt.% CaO. It should correspond to a quench glass phase.

5. Shock-induced physicochemical conditions associated with shock facies

The Yanzhuang meteorite underwent heterogeneous shock compression in an asteroid impact event. According to the shock metamorphism characteristics of the chondrite and the shock pressure calibration of chondrites by Stöffler *et al.* (1988, 1991), the weakly deformed chondritic host of Yanzhuang should have experienced shock pressures of 20 to 30 GPa and post-shock temperatures of 150 to 350°C; the brecciated areas, 30 to 40 GPa and 350 to 850°C; the blackened and partially melted areas, 50 to 90

GPa and 850 to 1300°C; shock-induced melt phase, ≥ 90 GPa and $\geq 1500^\circ\text{C}$. The heavily shock-metamorphosed areas (brecciated areas, blackened and partially melted areas, and melt phase) make up about 60 % by volume of the meteorite. It is clear that the meteorite underwent very high shock pressures and post-shock temperatures in most areas. Comparing the shock metamorphism intensity of Yanzhuang with other shocked chondrites, it appears that Yanzhuang is an example of the most severely shocked chondrites (Xie *et al.*, 1991).

The cooling rates of melt phase of the Yanzhuang have been estimated to be very fast; *i.e.* 100-400°C/s in the melt veins and 6-30°C/s in the melt pockets in the temperature interval 950-1400°C/s (Chen *et al.*, 1995).

6. Na behaviour in the melt phase

Average H-chondrite and L-chondrite falls contain 0.86 wt.% and 0.95 wt.% Na₂O respectively (Jarosewich, 1990). Na is easily mobilized from minerals by vaporization during heating. Experimental vaporization of the Holbrook L6 chondrite showed that Na vaporization occurs at 800-1250°C (Gooding & Muenow, 1977). However, Na mobilization in shocked and reheated meteorites may be affected by some other factors: (1) Pressure and temperature gradients. The movement of vapour from hotter to cooler areas (Fruiland, 1975) and from high pressure to low pressure areas would result in volatile depletion in the hotter and higher pressure areas; (2) Porosity of chondrite. Low rock porosity induced by shock compression would not be available as a mechanism for the mobilization of vapour phases; (3) Cooling rate. The rapid cooling or quenching of a shocked meteorite would prevent loss of most volatiles (Olsen, 1981).

The shock pressures and post-shock temperatures in the brecciated, blackened and partially melted areas, as well as the melt phase of Yanzhuang were high enough to release Na from minerals into the vapour phase. However, not only Na but also other volatile non-noble gas elements such as Zn, Se and K were not lost from the melt phase. Three explanations can be given for the Na retention: (1) the melt phase is surrounded by the high pressure and high temperature shock facies, so both the blackened and partially melted areas as well as the brecciated areas had lower temperature and pressure gradients and thus the

Na vapour could not be transported quickly from the melt phase to the surrounding areas. (2) shock compression reduced the meteorite porosity, especially in the severely metamorphosed facies, thus preventing most volatile elements in the melt phase from mobilization. (3) The cooling rates of melt phase of Yanzhuang were very fast (6 to 400°C/s). Fast cooling of melt phases reduced the mobilization of volatile elements and froze these elements into the solid phase.

Although there is no evident depletion of sodium in the melt phase of Yanzhuang, Na redistribution has taken place. Firstly Na along with other volatile elements such as Mn and P (or PO₄⁻³) concentrated into the Fe-Ni-S melt at high pressures and high temperatures. During rapid cooling, P, on the one hand, was solidified in metal dendrites as solid solutions (Chen *et al.*, 1995); while on the other hand, P, Fe, Mn, and Na crystallized as Fe-Mn and Fe-Mn-Na phosphates. Secondly, minor amounts of Na were solidified into crystallized low-Ca pyroxene, resulting in a slightly enhanced Na-content in the pyroxenes. Thirdly, the remaining Na was frozen into the silicate melt glass.

Conclusions

Four shock facies typical of disequilibrium shock effects can be distinguished in the Yanzhuang meteorite. Severely shocked facies including brecciated areas, blackened and partially melted chondritic areas, along with the melt phase, make up 60 % by volume of the meteorite. This shows that the meteorite underwent very high shock pressures (≥ 30 GPa) and post-shock temperatures in most areas, supporting the hypothesis that Yanzhuang is one of most severely shocked examples of ordinary chondrites.

There is no evident Na depletion in the melt phase of Yanzhuang. In this heavily shocked chondrite, reduced rock porosity, lower pressure and post-shock temperature gradients between melt phase and surrounding shock facies, as well as quenching of the melt phase (6-400°C/s), could be important factors in preventing loss of sodium from the melt phase.

During the shock event, Na redistribution in the melt phase occurred in the following ways: (1) Na concentrated into the Fe-Ni-S melt at high pressures and high temperatures, forming Fe-Mn-Na phosphate in metal-troilite eutectic

nodules. Due to sodium volatility and fast cooling, Fe-Mn-Na phosphate usually occurs in association with Fe-Mn phosphate forming mixture phase inclusions in troilite. (2) Minor amounts of Na were solidified into the recrystallized low-Ca pyroxene, resulting in a slightly higher Na content in the pyroxene; (3) Quenching of the melt resulted in that part of Na being frozen in the silicate melt glass.

It is concluded that Na behaviour in the shock facies of chondrites is an useful indicator in understanding the shock metamorphism of meteorites and the physicochemical conditions induced by shock waves.

Acknowledgements: This study was funded by the Guangdong Science Foundation of China, and partially supported by CAS and MPG through a joint research project on the study of Yanzhuang chondrite.

References

- Begemann, F., Palme, H., Spettel, B., Weber, H.W. (1992): On the thermal history of heavily shocked Yanzhuang H-chondrite. *Meteoritics*, **27**, 174-178.
- Chen Ming (1992): Micromineralogy and shock effects in Yanzhuang chondrite (H6). Ph.D. thesis, The Institute of Geochemistry, Chinese Academy of Sciences, 95p.
- Chen Yongheng, Dai Chengda, Wang Daode, Xie Xiande, Li Zhaohui, Fang Hong, Chai Zhifang (1994): Chemical compositions and shock effects of heavily shocked chondrites. *Geochemica*, **23**, 25-32.
- Chen Ming, Xie Xiande, El Goresy, A. (1995): Non-equilibrium solidification and microstructures of metal phases in the shock-induced melt of Yanzhuang (H6) chondrite. *Meteoritics*, **30**, 28-32.
- Dodd, R.T. & Jarosewich, E. (1982): The compositions of incipient shock melts in L6 chondrites. *Earth Planet. Sci. Lett.*, **59**, 355-363.
- Dodd, R.T., Jarosewich, E., Hill, B. (1982): Petrogenesis of complex veins in the Chantonay (L6f) chondrite. *Earth Planet. Sci. Lett.*, **59**, 364-374.
- Ferland, R.M. (1975): Volatile movement in Rose City meteorite, and implications concerning the impact and late thermal history of ordinary chondrites. *Meteoritics*, **10**, 403-404.
- Fuchs, L.H. (1969): The phosphate mineralogy of meteorites. in "Meteorite Research", P.M. Millman, ed. D. Reidel Publishing Company, Dordrecht-Holland, 683-695.
- Gooding, J.L. & Muenow, D. (1977): Experimental vaporization of the Holbrook chondrite. *Meteoritics*, **12**, 401-408.
- Jarosewich, E. (1990): Chemical analyses of meteorites: A compilation of stony and iron meteorite analyses. *Meteoritics*, **25**, 323-337.
- Olsen, E. (1981): Vugs in ordinary chondrites. *Meteoritics*, **16**, 45-59.
- Olsen E. & Steele, I. (1993): New alkali phosphates and their associations in the IIIAB iron meteorites. *Meteoritics*, **28**, 415.
- , — (1994): Lithophile element diffusion profiles in phosphate phases in IIIAB iron meteorites: a clue to the trace lithophiles in metal during core formation. *Lunar Planet. Sci.* **XXV**, 1025-1026.
- Semenenko, V.P. & Golovko, N.V. (1994): Shock-induced black veins and organic compounds in ordinary chondrites. *Geochim. Cosmochim. Acta*, **58**, 1525-1535.
- Semenenko, V.P., Kolesov, G.M., Ljul, A.Yu. (1992): Composition and structure of black veins in Barbotan (H5) and Charsonville (H6) chondrites. *Lunar Planet. Sci.* **XXIII**, 1263-1264.
- Stöffler, D., Bischoff, A., Buchwald, V., Rubin, A.E. (1988): Shock effects in meteorites. in "Meteorites and the Early Solar System", J.F. Kerridge and M.S. Matthews, ed. Univ. of Arizona Press, 165-202.
- Stöffler, D., Keil, K., Scott, E. D. (1991): Shock metamorphism of ordinary chondrites. *Geochim. Cosmochim. Acta*, **55**, 3945-3867.
- Xie Xiande, Li Zhaohui, Wang Daode, Liu Jingfa, Hu Ruiying, Chen Ming (1991): The new meteorite fall of Yanzhuang, a severely shocked H6 chondrite with black molten materials. *Meteoritics*, **26**, 411.
- , —, —, —, — (1994): The new meteorite fall of Yanzhuang, a severely shocked H6 chondrite with black molten materials. *Chinese J. Geochem.*, **13**, 39-45.

Received 1 December 1994

Modified version received 30 March 1995

Accepted 26 October 1995

